ELSEVIER

Contents lists available at ScienceDirect

Chemical Engineering Journal

journal homepage: www.elsevier.com/locate/cej



Enhanced ferrate(VI) oxidation of micropollutants in water by carbonaceous materials: Elucidating surface functionality



Bao Pan^{a,b}, Mingbao Feng^a, Thomas J. McDonald^a, Kyriakos Manoli^a, Chuanyi Wang^c, Ching-Hua Huang^{d,*}, Virender K. Sharma^{a,*}

- ^a Program for the Environment and Sustainability, Department of Environment and Occupational Health, School of Public Health, Texas A&M University, 212 Adriance Lab Rd, College Station TX 77843, USA
- b School of Chemistry and Chemical Engineering, Shaanxi University of Science and Technology, Xi'an 710021, PR China
- ^c School of Environmental Science and Engineering, Shaanxi University of Science and Technology, Xi'an 710021, PR China
- d School of Civil and Environmental Engineering, Georgia Institute of Technology, Atlanta, GA 30332, USA

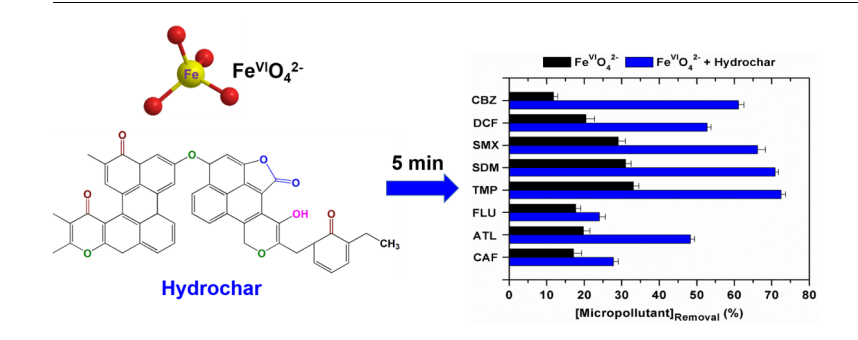
HIGHLIGHTS

- Carbonaceous solid-induced enhancement in oxidation of pharmaceuticals by ferrate.
- Carbonyl groups at surfaces of hydrochar and graphene oxide involve in enhancement.
- Magnitude of enhanced oxidation depends on moieties of micropollutant.
- Increased amounts of generated Fe^V/ Fe^{IV} result in increased oxidation.
- Hydrochar has superior reusability in activating Fe^{VI}O₄²⁻ to oxidize micropollutant.

ARTICLE INFO

Keywords:
Ferrate(VI)
Carbonaceous materials
Water micropollutants
Enhanced remediation
High-valent iron-oxo intermediates

GRAPHICAL ABSTRACT



ABSTRACT

Metal-free carbonaceous materials have increasingly attracted worldwide attention owing to their unprecedented properties in catalytic elimination of environmental pollutants in water. Nevertheless, the surface functionality-dependent catalytic efficacy and activation mechanism for ferrate(VI) ($Fe^{VI}O_4^{2-}$), an emerging green water-treatment agent, have remained largely unknown. Here we have examined if different carbonaceous materials (i.e., hydrochar, graphene oxide (GO), reduced graphene oxide, graphite, and fullerene) can activate $Fe^{VI}O_4^{2-}$ and enhance its effectiveness for rapid oxidation of a wide range of micropollutants (i.e., carbamazepine (CBZ), diclofenac, sulfamethoxazole, sulfadimethoxine, trimethoprim, flumequine, atenolol, and caffeine) under mild alkaline conditions. For example, the addition of hydrochar or GO into the reaction system, at pH 9.0, achieved remarkable enhancement of degradation of CBZ as compared to insignificant effect observed for three other carbonaceous materials. The magnitude of enhancement varied with the moieties of micropollutants. The Fourier-transform infrared spectroscopy (FTIR) technique in conjunction with the chemical probe (i.e., methyl phenyl sulfoxide) tests demonstrated chemical interactions of surface C=O groups of hydrochar with $Fe^{VI}O_4^{2-}$, of which high-valent iron-oxo intermediates (i.e., Fe^{IV}/Fe^V) were generated as the oxidizing species for enhanced remediation. Additionally, this enhancement was seen in five successive catalytic runs, indicating high recycl-

E-mail addresses: ching-hua.huang@ce.gatech.edu (C.-H. Huang), vsharma@tamu.edu (V.K. Sharma).

^{*} Corresponding authors.

ability of hydrochar to oxidize micropollutants by ${\rm Fe^{VI}O_4}^{2-}$. These findings suggest that heterogeneous carbonaceous activation of ${\rm Fe^{VI}O_4}^{2-}$ holds promise for advancing water remediation under mild alkaline reaction conditions.

1. Introduction

Iron is abundantly available globally and is the basic metal in numerous industrial applications in modern society. Iron in low-valent oxidations states (i.e., Fe(0), Fe(II), and Fe(III)) is driving progress in technology such as molecular electronics, nanotechnology, material science, and chemodynamic cancer therapy [1,2]. Iron in high-valent states (Fe^{IV}, Fe^V, and Fe^{VI}) have gained increasing interest due to their participation in metalloenzymes, biological science, and environmental remediation [3-6]. High-valent iron-imido and iron-oxo complexes have been proposed as key reactive intermediates in metabolic oxidative biotransformation [7,8]. In environmental processes, high-valent compounds including Fe^{IV}/Fe^V-TAML complex (TAML = tetra-amido macrocyclic ligands) and ferrate(VI) (FeVIO42-) have shown great potentials to degrade a wide range of micropollutants [9-12]. Many investigations on the properties of FeVIO42- as an oxidant, disinfectant, and coagulant have been conducted [13-18]. It has been observed that the rates of the reactions of $\mathrm{Fe^{VI}O_4}^{2-}$ with micropollutants decreased with pH, and in some instances, the reactivity is sluggish (i.e., degradation occurs in hours) [19-22]. Generally, the second-order rate constants of the reactions are decreased significantly when the pH of the solution is increased from neutral pH to slightly alkaline pH (e.g., from pH 7.0 to 9.0) [11,23,24]. Therefore, in the last few years, many researchers including our laboratory studied different approaches to accelerate the oxidation process in order to degrade such pollutants efficiently by Fe^{VI}O₄²⁻ in slightly alkaline medium [10,25-28]. In other words, oxidative elimination of organic micropollutants could be achieved in seconds/minutes instead of hours.

Initially, the studies were conducted using various reducing substrates (R) in combination with Fe^{VI}O₄²⁻ to accelerate the oxidation of micropollutants [10,29–31]. The reducing ions could produce Fe^{IV}/Fe^V, which have 2–4 orders of magnitude higher reactivity than Fe^{VI}O₄^{2–} to remove the target pollutants in seconds [32–34]. Among the various R, researchers have focused on using sulfite (S(IV)) to oxidize micropollutants rapidly in 15-30 s and demonstrated involvement of intermediate Fe^{IV}/Fe^{V} species in the $Fe^{VI}O_4^{2-}$ -R systems [29,30,35]. Besides reducing ions, phosphate, borate, bicarbonate, ammonia, and silica have also been investigated [36-38]. Interestingly, borate had no influence while phosphate showed inhibition of the oxidation by Fe^{VI}O₄²⁻ [25,36]. However, bicarbonate, ammonia, and silica have shown increased degradation of micropollutants due to the participation of Fe^{IV}/Fe^V species [37-39]. A recent study explored the use of carbon nanotubes (CNTs) to activate FeVIO42- to oxidize electron-rich pollutants [40]. The surface reducing groups such as phenolic hydroxyl of CNTs were explored to activate Fe(VI) to remove organic pollutants. This led us to ask the question whether other carbonaceous materials may also influence the oxidation of pollutants by Fe^{VI}O₄²⁻. Additionally, the possible effect of surface properties (e.g., morphology, surface area, and surface functional groups like alkyl carbonyl and carboxylic groups) of different carbonaceous nanomaterials on the activation of Fe^{VI}O₄²⁻ for water depollution is still unknown.

The objectives of this paper were (i) to evaluate and compare the efficiency of different carbonaceous materials (i.e., fullerene, graphite, graphene oxide (GO), reduced graphene oxide (rGO), and hydrochar) to enhance the oxidation of micropollutants by ${\rm Fe^{VI}O_4}^{2-}$ in slight alkaline medium, (ii) to learn the variation in enhanced degradation of micropollutants of different moieties (i.e., carbamazepine (CBZ), diclofenac (DCF), sulfamethoxazole (SMX), sulfadimethoxine (SDM), trimethoprim (TMP), flumequine (FLU), atenolol (ATL), and caffeine (CAF)) by ${\rm Fe^{VI}O_4}^{2-}$ -carbonaceous material system. The selected micropollutants

are widely present in the aquatic environment in the concentration range of ng/L-µg/L, and generally ${\rm Fe^{VI}O_4}^{2-}$ has sluggish reactivity with these molecules under alkaline conditions [19,28], (iii) to gain insight into the mechanism of observed enhanced oxidation by ${\rm Fe^{VI}O_4}^{2-}$ -carbonaceous materials compared to ${\rm Fe^{VI}O_4}^{2-}$ alone by applying Fouriertransform infrared spectroscopy (FTIR) technique and using the chemical probe (methyl phenyl sulfoxide (PMSO)) of iron intermediates (Fe^{IV}/Fe^V), and (iv) to study the recycling efficiency of carbonaceous materials to oxidize micropollutants in water.

2. Materials and methods

2.1. Chemicals and reagents

CBZ, ATL, CAF, DCF, FLU, SDM, SMX, TMP, phenyl sulfoxide (PMSO, 98%), methyl phenyl sulfone (PMSO2, 98%), D-Glucose monohydrate, sodium borate, and hydroxylamine (NH2OH) were purchased either from Fisher-Scientific (Austin, TX, USA) or Sigma-Aldrich (St. Louis, MO, USA). Graphite powder and fullerene were supplied from Oingdao Black Dragon Graphite Co., Ltd. (Oingdao, China) and Tokyo Chemical Industry Co. Ltd. (Tokyo, Japan), respectively. Methanol used in the high-performance liquid chromatography (HPLC) was obtained from Fisher-Scientific (Austin, TX, USA). Potassium ferrate (K₂FeO₄, purity > 95%) was synthesized in our lab via wet chemical method [41]. All solutions were prepared using deionized (DI) water from a purification system (18.0 M Ω cm, Milli-Q Millipore, Waters Alliance, Milford, MA, USA). Stock solutions of FeVIO42- were freshly prepared by dissolving solid K₂FeO₄ in buffer solutions (10.0 mM borate at pH 9.0) and the levels were quantified by the direct absorbance measurements at 510 nm ($\epsilon_{510nm} = 1150 \, \text{M}^{-1} \, \text{cm}^{-1}$) [42]. The measurements were performed using an UV-visible spectrometer (DR-5000, Hach Co., USA). Sonication of the carbonaceous materials in DI water was applied to prepare the stock suspensions, which were subjected to sonication for 5 min prior to each experiment.

2.2. Synthesis of carbonaceous materials

GO was synthesized via the modified Hummers' method. Briefly, 1.0 g powder graphite and 0.5 g NaNO $_3$ were mixed with 23 mL concentrated $\rm H_2SO_4$ in a 500-mL flask placed in an ice-water bath. The obtained solution was stirred and slowly added with 3.0 g potassium permanganate. The mixed solution was continuously stirred for 2 h, and then transferred to a 35 °C water bath and stirred for 30 min. Afterwards, 50 mL of DI water was slowly added into the solution and the temperature was maintained at 98 °C for 30 min. Subsequently, 100 mL DI water and 10 mL $\rm H_2O_2$ were added sequentially to the mixed solution to terminate the reaction. The resulting product was filtered and rinsed with 10% HCl and DI water. The GO powder was obtained after drying at 60 °C for 10 h.

Typically, for the reduction of GO to rGO, 50 mg GO was dispersed in 35 mL DI water by ultrasonic treatment for 1 h to yield a yellow—brown solution. The pH of the GO dispersion was adjusted to 10.0 using 20% ammonia solution. After stirring for 1.0 h, the resultant aqueous suspension was transferred to a 50.0 mL Teflon-lined stainless-steel autoclave and subjected to hydrothermal treatment at 180 $^{\circ}$ C for 6.0 h. The resulted product was collected by centrifugation, washed with water, and dried at 60 $^{\circ}$ C (denoted as rGO).

In synthesizing hydrochar, 2.5 g glucose was dissolved in 35 mL deionized (DI) water. The reaction mixture was then sealed into a stainless-steel autoclave with 50.0 mL capacity and hydrothermally

treated at 180 °C for 10 h. The solid product was recovered by vacuum filtration and washed with water and ethanol several times, and finally dried at 60 °C under vacuum overnight. The obtained biochar from glucose was denoted as hydrochar based on the synthetic approach (i.e., hydrothermal carbonization) [43,44].

2.3. Oxidation of micropollutants by $Fe^{VI}O_4^{\ 2-}$ in the absence/presence of carbonaceous materials

Oxidation experiments were conducted in 50 mL beaker at 25 ± 1 °C with magnetic stirring. Experiments were performed at pH 9.0 (10.0 mM borate buffer). The hydrolyzed human urine samples (one of the important pollution sources of different pharmaceuticals) have a solution pH of ~ 9.0 [36]. Our study may facilitate the applications of the studied system in remediating the urine samples and natural waters under alkaline conditions. Unless otherwise specified, the reactions were initiated by adding K₂FeO₄ (100.0 μM) into pH-buffered solutions containing CBZ (5.0 μ M) and carbonaceous materials (50.0 mg/L). At designated intervals, 1.0 mL samples were withdrawn, quenched with 20.0 µL of 1.0 M hydroxylamine (NH₂OH), and filtered through 0.45 µm polypropylene membrane to measure residual CBZ using a HPLC method. The effect of Fe^{VI}O₄²⁻ concentrations (i.e., 10.0, 100.0, 150.0, and 200.0 μM) and dosages of carbonaceous materials (i.e., 10.0, 20.0, 50.0, and 100.0 mg/L) was investigated at pH 9.0. To evaluate the adsorption efficiency of CBZ by carbonaceous materials, the solutions were mixed in the absence of Fe^{VI}O₄²⁻, and the samples collected at the same time intervals were filtered to perform HPLC analysis. Similar removal experiments were also performed for seven other micropollutants (i.e., SDM, TMP, SMX, DCF, CAF, FLU, and ATL; 5.0 μ M for each compound) by Fe^{VI}O₄ $^2-$ (100.0 μ M) and hydrochar/GO (50.0 mg/ L) at pH 9.0. All experiments were conducted with at least triplicates. The mean values and standard deviations were reported.

2.4. Analytical methods

An Ultimate 3000 Ultra high performance liquid chromatography (UHPLC) (ThermoFisher Scientific), equipped with a RESTEK Ultra C_{18} analytical column (4.6 \times 250 mm, particle size 5 μm) and a diode array detector (set up at 284 nm), was used for quantifying the concentrations of CBZ. The column temperature was set at 30 °C. A 0.05% phosphoric acid in water (A) and methanol (B) were used as mobile phase at a flow rate of 0.80 mL/min. The injection volume was 20 μL , and the mobile phase composition of A and B was 30% and 70%, respectively. The detailed HPLC conditions for seven other micropollutants (i.e., SDM, TMP, SMX, DCF, CAF, FLU, and ATL) are provided in Table SM-1.

FTIR spectra were recorded using a Nicolet iS50 FTIR Spectrometer (Thermo Fisher Scientific Co., Waltham, MA, USA). After 30 min of oxidation, the carbonaceous materials were filtrated from the reaction solution using 0.45 μm membrane filter (Gelman Sciences), dried at 60 °C under vacuum, and then reused in a freshly prepared reaction mixture for five cyclic runs. FTIR spectra of the used samples were collected after each cyclic operation. The X-ray photoelectron spectroscopy (XPS) measurements were carried out using an AXIS ULTRA DLD X-ray photoelectron spectrometer with an excitation source of Al $K\alpha=1486.6$ eV. The prepared hydrochar and GO powders were characterized by XPS analysis.

3. Results and discussion

3.1. Degradation of CBZ

Initial studies were conducted using CBZ as a model micropollutant. CBZ is a dibenzoazepine that carries a substituent at the nitrogen of unsaturated heterocycles of seven atoms (Fig. SM-1). The degradation of CBZ was monitored as a function of time for 30 min with and without ${\rm Fe^{VI}O_4}^{2-}$ in the presence of five carbonaceous materials (CMs) (i.e.,

GO, hydrochar, rGO, graphite, and fullerene) (Fig. 1). The adsorption of CBZ by CMs only (i.e., without ${\rm Fe^{VI}O_4}^2$) was below 10%, except for rGO (Fig. 1a). The adsorption of CBZ onto rGO was up to \sim 40%.

The degradation of CBZ by ${\rm Fe^{VI}O_4}^{2-}$ in the presence of CMs is presented in Fig. 1b. The removal of CBZ by ${\rm Fe^{VI}O_4}^{2-}$ was only 30%. However, the presence of GO, hydrochar, and rGO enhanced the removal of CBZ by ${\rm Fe^{VI}O_4}^{2-}$. The graphite and fullerene had no effect on removing CBZ. The complete elimination of CBZ could be seen in the use of GO and hydrochar in 30 min (Fig. 1b). Comparatively, rGO showed modest enhancement from $\sim 40\%$ (CBZ-rGO alone) to $\sim 50\%$ (CBZ-Fe^{VI}O₄²⁻-rGO) (Fig. 1b). Results in Fig. 1b suggest that the CMs like GO and hydrochar could produce additional oxidative reactive species to enhance the degradation of CBZ (see later discussion). However, no such species could exist in the reaction solution of CBZ-Fe^{VI}O₄²⁻-CMs (CM = rGO, graphite, and fullerene) to cause any enhancement in oxidation of CBZ by ${\rm Fe^{VI}O_4}^{2-}$. Hence, the subsequent studies were conducted using GO and hydrochar as the target CMs.

Next, the effect of the concentration of ${\rm Fe^{VI}O_4}^{2-}$ on the degradation of CBZ was examined by keeping the concentration of GO or hydrochar as 50 mg/L (Fig. 2). An increase in concentration of ${\rm Fe^{VI}O_4}^{2-}$ increased the enhancement effects of GO and hydrochar (Fig. 2a-2d). It appears the increase in generation of oxidative reactive species with the increase in concentrations of ${\rm Fe^{VI}O_4}^{2-}$ to observe the results in Fig. 2 (see later discussion). Results further suggest that the concentration of the reactive oxidative species depended on the nature of CMs. Hydrochar had more enhancement than GO in the ${\rm Fe^{VI}O_4}^{2-}$ -CBZ solution. An example is presented in Fig. SM-2 on the difference in enhancement of the two CMs (GO and hydrochar) on the removal of CBZ in 5 min at various concentrations of ${\rm Fe^{VI}O_4}^{2-}$. Complete elimination of CBZ by 200.0 μ M ${\rm Fe^{VI}O_4}^{2-}$ required 10 min when hydrochar was used (Fig. 2d).

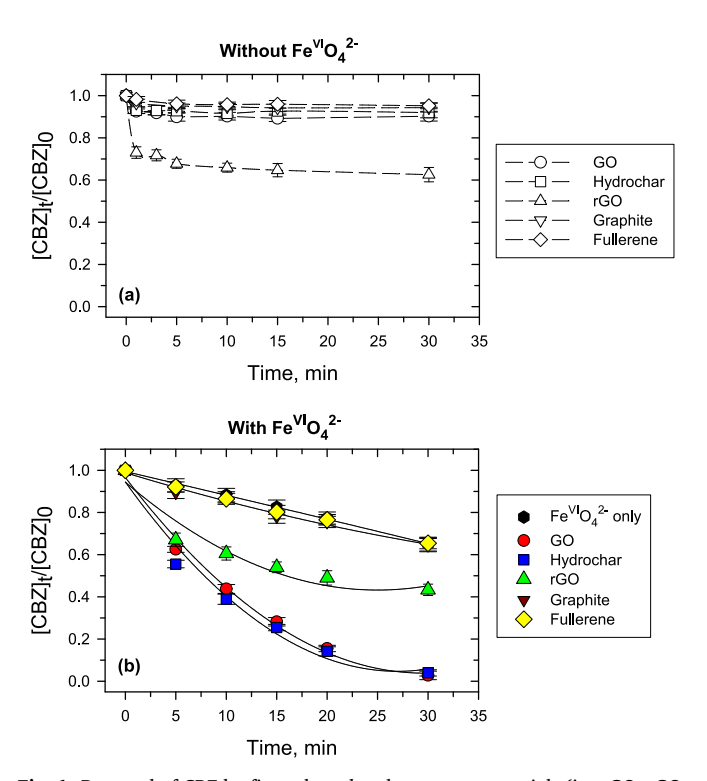


Fig. 1. Removal of CBZ by five selected carbonaceous materials (i.e., GO, rGO, hydrochar, Graphite, and Fullerene) with and without ${\rm Fe^{VI}O_4}^{2-}$ at pH 9.0. (a) Carbonaceous materials, (b) carbonaceous materials and ${\rm Fe^{VI}O_4}^{2-}$. (Experimental conditions: ${\rm [CBZ]_0}=5.0~\mu{\rm M},~{\rm [Fe^{VI}O_4}^{2-}]_0=100.0~\mu{\rm M},~{\rm [GO]_0}={\rm [rgO]_0}={\rm [hydrochar]_0}={\rm [Graphite]_0}={\rm [Fullerene]_0}=50.0~{\rm mg/L},~10.0~{\rm mM}$ borate buffer, T = 25.0 \pm 1.0 °C). Note: CBZ, carbamazepine; GO, graphene oxide; rGO, reduced graphene oxide; Hydrochar, carbonization of glucose.

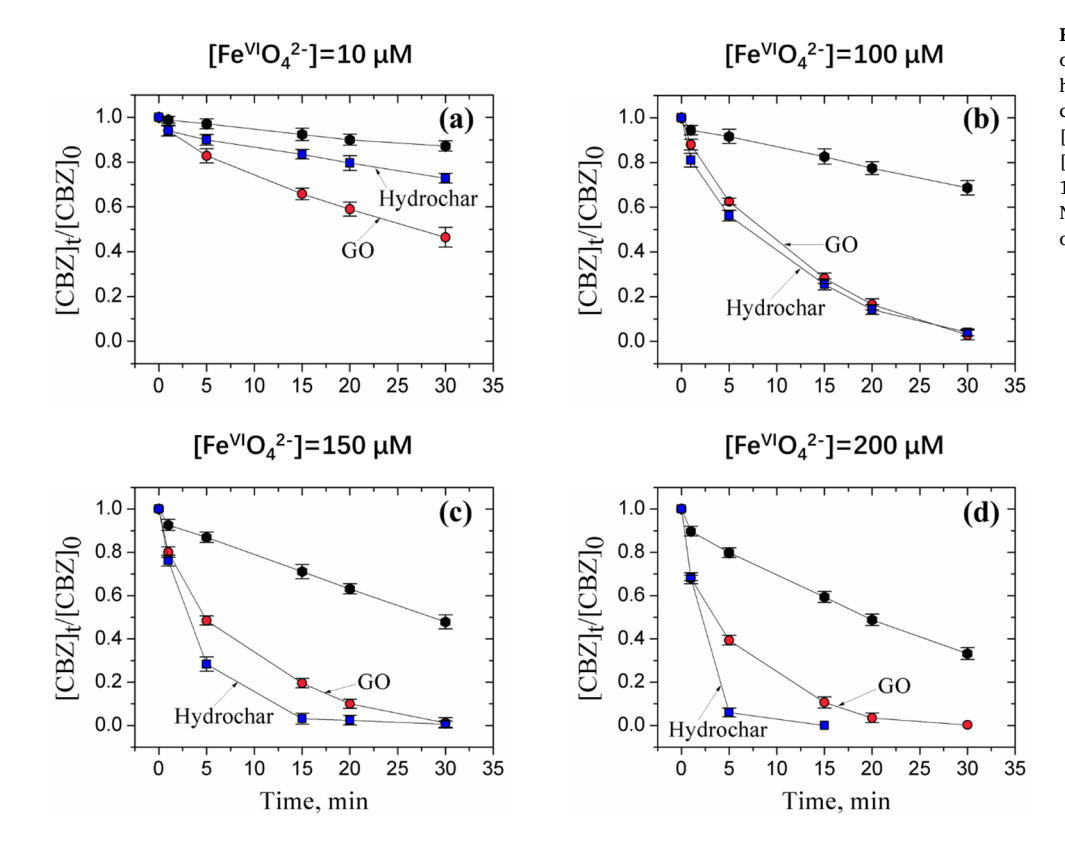


Fig. 2. Effect of ${\rm Fe^{VI}O_4}^2$ concentration on the removal of CBZ by GO and hydrochar at pH 9.0. (Experimental conditions: ${\rm [CBZ]_0}=5.0~\mu{\rm M}, {\rm [Fe^{VI}O_4}^2-{\rm]}_0=10.0-200.0~\mu{\rm M}, {\rm [GO]_0}={\rm [hydrochar]_0}=50.0~{\rm mg/L}, 10.0~{\rm mM}~{\rm borate~buffer}, T=25.0~\pm~1.0~{\rm °C}).$ Note: CBZ, carbamazepine; GO, graphene oxide; Hydrochar, carbonization of glucose.

However, when GO was used, 30 min was needed to achieve nearly complete removal of CBZ (Fig. 2d).

Finally, the amount of GO and hydrochar in Fe^{VI}O₄²⁻-CBZ solution was varied by keeping concentration of Fe^{VI}O₄²⁻ constant at 100.0 μM to investigate the effect of CMs on the degradation of CBZ (Fig. 3). The varied amount from 20.0 to 100.0 mg/L of only hydrochar in solution did not adsorb (or remove) CBZ (Fig. SM-3). The degradation of CBZ by oxidation in the FeVIO₄²⁻-CMs system depended on the amount of GO or hydrochar. Results showed the complete oxidation of CBZ within 30 min in the presence of GO at 50.0 mg/L (Fig. 3a). The amount greater than 50.0 mg/L (i.e., 100.0 mg/L) had no further enhancement (Fig. 3a). Comparatively, only 20.0 mg/L of hydrochar was needed in the presence of Fe^{VI}O₄²⁻ to eliminate CBZ (Fig. 3b). Furthermore, high amount of 100.0 mg/L hydrochar inhibited the oxidation of CBZ (Fig. 3b). It seems that this high concentration could have dominance of self-decomposition of ferrate species over the reactions of ferrate species with CBZ to observe such inhibition (more is discussed in section 3.3). Overall, these results are consistent with the observation on the oxidation of CBZ in Fig. 2 at different concentrations of FeVIO42- in presence of CMs. Basically, enhanced removal of CBZ by the Fe^{VI}O₄²⁻-CMs system occurred at optimum concentrations of Fe^{VI}O₄²⁻ and CMs (i.e., 50.0 mg/L) in solution.

3.2. Degradation of micropollutants

Studies conducted using CBZ were extended to other micropollutants (DCF, SMX, SDM, TMP, CAF, FLU, and ATL) (Fig. SM-1). DCF is a monocarboxylic acid consisting a (2,6-dichlorophenyl)amino group at the 2-position. SMX and SDM are sulfonamide antibiotics. TMP is an antibiotic containing a 2,4-diamino-5-(3',4',5'-trimethoxybenzyl) pyrimidine molecule. FLU is a synthetic fluoroquinolone antibiotic. ATL is a beta-blocker and a molecule may be described as benzeneacetamide. Molecular structure of caffeine is 1,3,7-trimethylxanthine (Fig. SM-1). First, the adsorption of the micropollutants onto GO and hydrochar was examined (Fig. 4). Most of the micropollutants either had no adsorption

or low removal by these two CMs (Fig. SM-4). The removal of the studied micropollutants by the adsorption processes onto CMs under alkaline medium may be understood by considering polar characteristic of these contaminants and the generally non-polar nature of CMs [45–47].

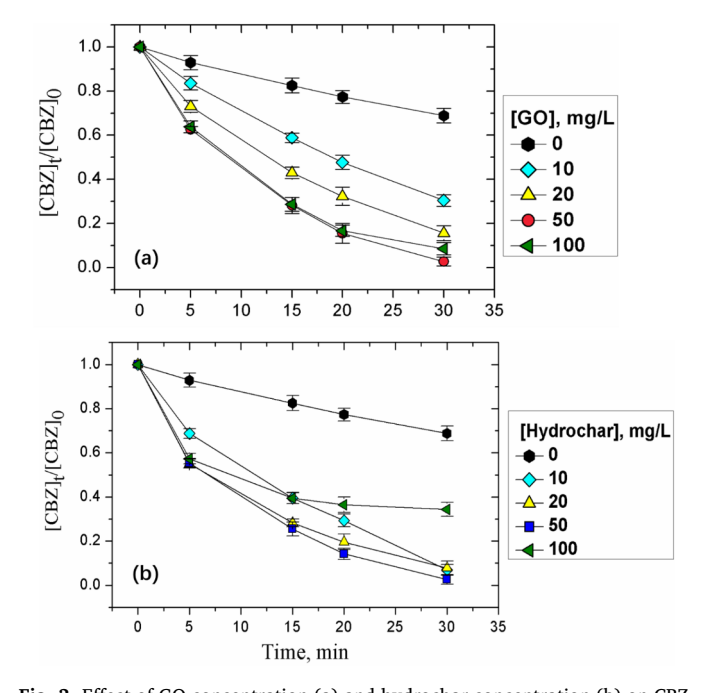


Fig. 3. Effect of GO concentration (a) and hydrochar concentration (b) on CBZ removal by Fe^{VI}O₄ 2 . (Experimental conditions: [CBZ] $_0=5.0~\mu\text{M}$, [Fe^{VI}O₄ 2] $_0=100.0~\mu\text{M}$, [GO] $_0=[\text{hydrochar}]_0=0$ –100.0 mg/L, 10.0 mM borate buffer, T = 25.0 \pm 1.0 °C). Note: CBZ, carbamazepine; GO, graphene oxide; Hydrochar, carbonization of glucose.

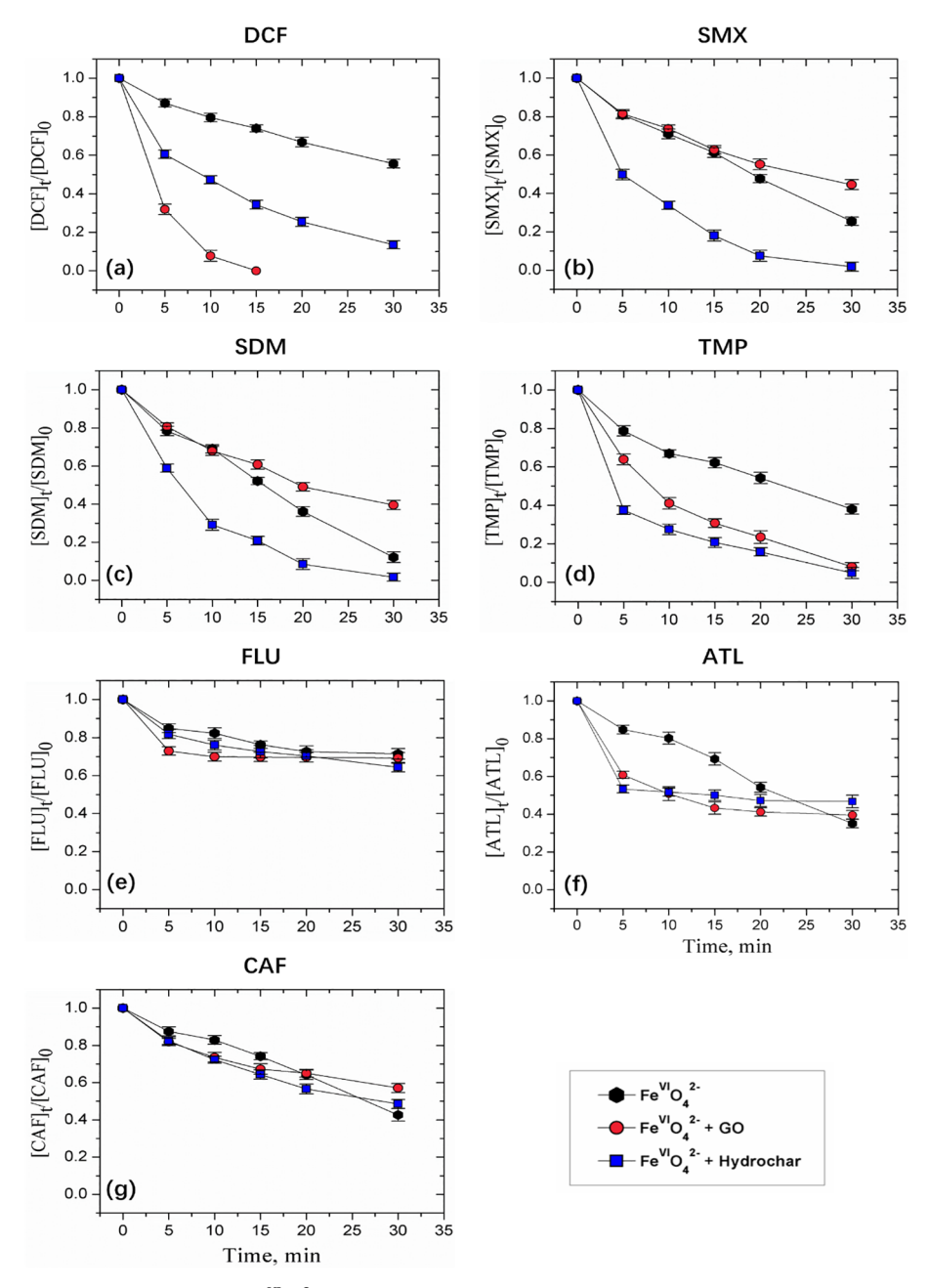


Fig. 4. Removal of a variety of micropollutants by $Fe^{VI}O_4^{2-}$ in solution containing carbonaceous. (Experimental conditions: [Micropollutant]₀ = 5.0 μM, $[Fe^{VI}O_4^{2-}]_0 = 100.0 \,\mu\text{M}$, $[GO]_0 = [hydrochar]_0 = 50.0 \,mg/L$, 10.0 mM borate buffer, $T = 25.0 \pm 1.0 \,^{\circ}\text{C}$). Note: GO, graphene oxide; Hydrochar, carbonization of glucose; DCF, diclofenac; SMX, sulfamethoxazole; SDM, sulfadimethoxine; TMP, trimethoprim; FLU, flumequine; ATL, atenolol; CAF, caffeine.

The effect of the GO and hydrochar on the removal of the micropollutants by ${\rm Fe^{VI}O_4}^{2-}$ is presented in Fig. 4. The enhanced effects of the CMs on the oxidation of DCF, SMX, SDM, and TMP were found (Fig. 4a-4d). Significantly, the observed results for SMX, SDM, and TMP were more pronounced in the use of hydrochar than that of applying GO. In the case of DCF, GO exhibited higher enhancement than hydrochar (Fig. 4a). The oxidation of FLU, ATL, and CAF, by ${\rm Fe^{VI}O_4}^{2-}$ could not be increased by either hydrochar or GO (Fig. 4e-4g). Results of Fig. 4 indicate the possible role of the structure of micropollutants in CM-induced oxidation of target pollutants by ${\rm Fe^{VI}O_4}^{2-}$. Basically, ferrate species have a trend of reactivity as $\alpha\text{-C-NH}_2 > \alpha\text{-C-OH} > \alpha\text{-C-H}$ [48,49]. This suggests the role of moieties present in the structures of pollutants to be oxidized by the ferrate species.

3.3. Mechanistic insight

The trend of the influence of CMs on the oxidation of micropollutants by ${\rm Fe^{VI}O_4}^{2-}$ may be interpreted by considering the structures of CMs and possible sequence of reactions that may take place in the mixture of CMs-Fe^{VI}O₄²⁻-micropollutant (X) (Reactions (R1)–(R8)).

$$2Fe^{VI}O_4^{2-} + H_2O \rightarrow 2Fe^{IV}O_3^{2-} + O_2 + H_2O$$
 (R1)

$$Fe^{VI}O_4^{\ 2-} + H_2O + Cat-CM \rightarrow Fe^{IV}/Fe^V + O_2$$
 (R2)

$$\text{Fe}^{\text{VI}}\text{O}_4{}^{2-} + \text{Carbonyl/carboxyl-CM} \rightarrow \text{Fe}^{\text{IV}}/\text{Fe}^{\text{V}} + \text{Product(s)}$$
 (R3)

$$Fe^{IV}/Fe^{V} + H_2O \rightarrow Fe^{III} + O_2$$
 (R4)

$$Fe^{IV}/Fe^{V} + H_2O + Cat-CM \rightarrow Fe^{III} + O_2$$
 (R5)

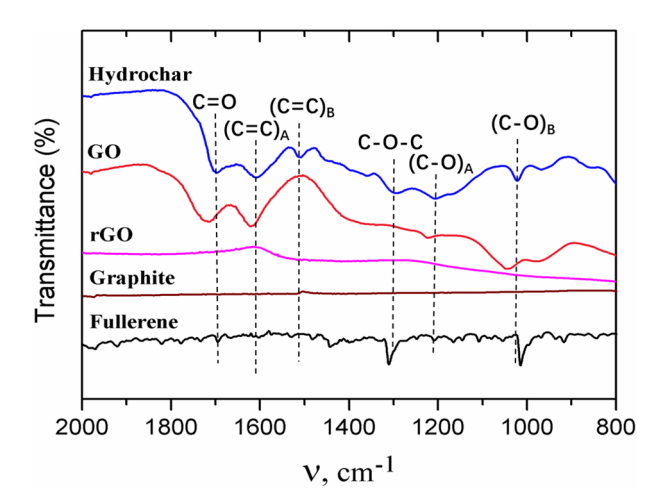


Fig. 5. FTIR of hydrochar, GO, rGO, Graphite, and Fullerene.

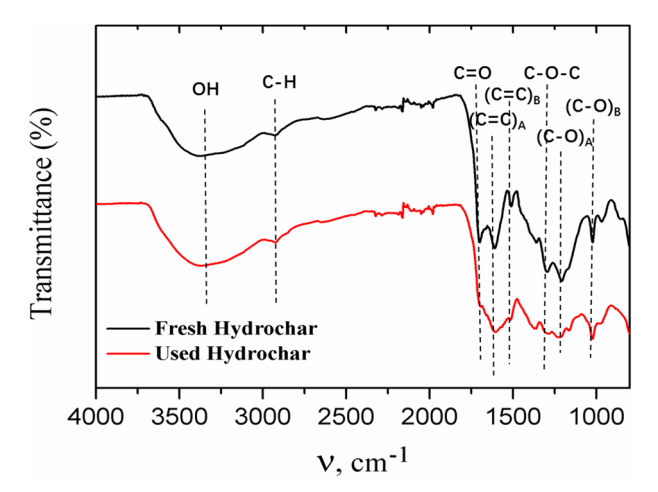


Fig. 6. FTIR of the fresh and used hydrochar.

$$Fe^{IV}/Fe^{V} + Carbonyl/carboxyl-CM \rightarrow Fe^{III} + Product(s)$$
 (R6)

$$Fe^{VI}O_4^{2-} + X \rightarrow Fe^{III} + Oxidized Product(s) (OPs)$$
 (R7)

$$Fe^{IV}/Fe^{V} + X \rightarrow Fe^{III} + Oxidized Product(s) (OPs)$$
 (R8)

Degradation of ${\rm Fe^{VI}O_4}^{2-}$ in water may happen from three reactions, i.e., Reactions (R1)–(R3). In Reaction (R1), the decomposition of ${\rm Fe^{VI}O_4}^{2-}$ by water predominately occurs by first-order in mild alkaline medium to give ${\rm Fe^{IV}O_3}^{2-}$; evidenced by experimental and theoretical calculations [39,50]. The decay of ${\rm Fe^{VI}O_4}^{2-}$ in water may also be

catalyzed by CMs to form high-valent intermediates (Reaction (R2)). It is also possible that the functional groups present on the surfaces of the studied CMs would interact with ${\rm Fe^{VI}O_4}^{2-}$ (Reaction (R3)). As shown in Fig. 5 (the expanded FTIR spectra over a wider wavenumber range are shown in Fig. SM-5), FTIR characteristics showed different groups, which are of carbonyl/carboxyl nature. We have postulated that these groups would react with ${\rm Fe^{VI}O_4}^{2-}$ to yield ${\rm Fe^{IV}/Fe^V}$ species (Reaction (R3)), based on the literature of the reactivity of ${\rm Fe^{VI}O_4}^{2-}$ with carbonyl compounds [51,52]. The intermediate species are written as ${\rm Fe^{IV}/Fe^V}$ species because of not knowing their structures.

The ${\rm Fe^{IV}/Fe^V}$ species, produced in Reactions (R1)–(R3), could possibly go through reactions with water (without and with CMs, i.e., Reactions (R4) and (R5), respectively) and with carbonyl constituents of CMs (Reaction (R6)) [53–55]. Micropollutant (X) in the reaction mixture would also participate by reacting with all high-valent iron species (Reactions (R7) and (R8)); reactions responsible for enhancing the degradation of the target X. ${\rm Fe^{IV}/Fe^V}$ species have 2–4 orders of magnitude higher reactivity than ${\rm Fe^{VI}O_4}^{2-}$ [32,48]. Overall, the enhanced degradation of X by ${\rm Fe^{VI}O_4}^{2-}$ in presence of CMs would depend on the cumulative effects of Reactions (R1)–(R8). In other words, the generated ${\rm Fe^{IV}/Fe^V}$ species through Reactions (R1)–(R3) must preferably react with X (desired reactions) rather than their disappearance by Reactions (R4)–(R6) (un-desired reactions) to produce final reduced ${\rm Fe^{III}}$ species. This analogy can be applied to describe the results seen in Figs. 1–4.

Roles of different reactions in the degradation of X by the Fe^{VI}O₄²⁻CMs were examined by collecting FTIR spectra of different CMs (Fig. 5). In hydrochar, different peaks were observed at 3374, 2932, 1704, 1606, 1520, 1300, 1210, and 1021 cm⁻¹, which are assigned to OH, C–H, C=O, (C=C)_A, (C=C)_B, C–O–C, (C–O)_A, and (C–O)_B groups, respectively. These assignments are consistent with the proposed structure of hydrochar (Fig. SM-6a). In GO, C=O, C=C, and C–O are the functional groups, which are in agreement with the proposed structure of the molecule (Fig. SM-6b). These functional groups were not seen in rGO. Graphite has no functionality that can be observed by FTIR spectrum. The functional groups in fullerene are largely missing (Fig. 5).

The possible role of the functional groups on CMs was examined using hydrochar. In the solution of ${\rm Fe^{VI}O_4}^{2-}$ exposed to hydrochar after 30 min, the resulted dried solid was separated and then subjected to FTIR characterization. The comparison of the two spectra (fresh and after exposure to ${\rm Fe^{VI}O_4}^{2-}$) is shown in Fig. 6. Functional groups of fresh samples, investigated by XPS measurements, showed similar findings (see Fig. SM-7). The results of FTIR showed the disappearance of some functional groups (e.g., C=O) of the hydrochar after its exposure to ${\rm Fe^{VI}O_4}^{2-}$. This indicates the occurrence of the reaction between ${\rm Fe^{VI}O_4}^{2-}$ and functional groups present on the surface of hydrochar (i.e., envisioned Reaction (R6)), supported by independent

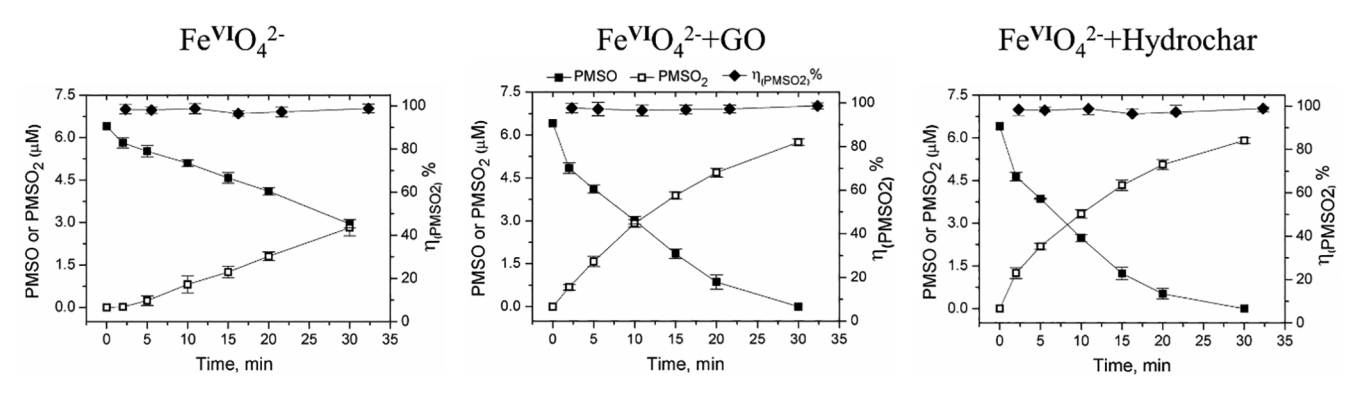


Fig. 7. The oxidation of PMSO and the generation of PMSO₂ and the calculated $\eta(PMSO_2)$ values in $Fe^{VI}O_4{}^{2-}$ and $Fe^{VI}O_4{}^{2-}$ -carbonaceous materials systems at pH 9.0. (Experimental conditions: $[PMSO]_0 = 6.5 \, \mu M$, $[Fe^{VI}O_4{}^{2-}]_0 = 100.0 \, \mu M$, $[GO]_0 = [hydrochar]_0 = 50.0 \, mg/L$, 10.0 mM borate buffer, $T = 25.0 \, \pm \, 1.0 \, ^{\circ}C$).

Table 1 Species-specific rate constants $(M^{-1} s^{-1})$ for the reaction between ferrate(VI) and micropollutants.

Pollutant	pK_a	$k(HFe^{VI}O_4^- + HX)$	$k(\text{Fe}^{\text{VI}}\text{O}_4^{\ 2^-} + \text{HX})$	$k(HFe^{VI}O_4^- + X^-)$	$k(\text{Fe}^{\text{VI}}\text{O}_4^{\ 2^-} + \text{X}^-)$	k_{app} (pH 9.0)
$(HX \rightleftharpoons H^+ + X^-)$	$(M^{-1} s^{-1})$	$(M^{-1} s^{-1})$	$(M^{-1} s^{-1})$	$(M^{-1} s^{-1})$	$(M^{-1} s^{-1})$	
CBZ ^a	_	_	_	1.1×10^{2}	9.0×10^{-1}	2.7
SMX^b	5.7 ^h	3.0×10^{4}	1.2	1.7×10^{2}	3.1	
SDM ^c	6.1 ⁱ	1.9×10^{4}	_	3.8×10^{2}	6.7	
TMP^d	7.2^{j}	8.5×10^{1}	2.5×10^{1} -	_	4.1×10^{-1}	
DCF ^e	4.2 ^k	_	_	2.1×10^{2}	1.5	1.2
FLU^f	6.5 ¹	_	_	_	_	1.2
ATL^g	9.6 ^m	2.0×10^{3}	-	-	$7.0 \times 10^{-1, n}$	

afrom [21]; bfrom [58]; ffrom [59]; afrom [60]; ffrom [21]; ffrom [37]; ffrom [61]; hfrom [62]; ffrom [63]; ffrom [64]; hfrom [65]; hfrom [65]; hfrom [65]; hfrom [66]; hfrom

investigations on the reactions between FeVIO42- and carbonyl/carboxyl group-containing compounds [51,52]. Furthermore, participation of Reactions (R4)-(R6) could also be seen in monitoring the decay of Fe^{VI}O₄²⁻ in water containing CMs (Fig. SM-8a). Decay of Fe^{VI}O₄²⁻ was found to be in increasing order as graphite ~fullerene < GO < hydrochar. This is in agreement with the FTIR spectra, in which hydrochar has the highest functionality (Fig. 5). The role of functionality could also be seen in increasing decay of Fe^{VI}O₄²⁻ with an increase in amount of hydrochar (Fig. SM-8b). In the case of GO, the functionality is decreased, hence the reduction in the decay of Fe^{VI}O₄²⁻ (Fig. SM-8a). The decay of FeVIO42- in water in the presence of graphite and fullerene was only slightly higher than that without these CMs, indicating almost no role of Reaction (R6). The difference in decays of Fe^{VI}O₄²⁻ in the presence of graphite and fullerene compared to their absence is due to some influences of solid surfaces, which could catalyze the reduction of Fe^{VI}O₄²⁻ in water via Reaction (R5). Overall, the participation of Reaction (R3) would be the highest in hydrochar to generate Fe^{IV}/Fe^V species that could react with target micropollutant, X, to cause its enhanced degradation (i.e., Reaction (R8)). The production of Fe^{IV}/Fe^V species seems to be the highest in the case of hydrochar, and therefore, could degrade CBZ at the fastest rate compared to other CMs (see Fig. 1b). Rates are proportionally dependent on the concentrations of reactants, and increasing concentrations of Fe^{IV}/Fe^V species in the reactive system would increase the degradation of CBZ. Similarly, increase in amounts of Fe^{VI}O₄²⁻ and hydrochar would result in increase in degradation of CBZ, generally consistent with the results of Figs. 2 and 3. GO had a lower rate of generating Fe^{IV}/Fe^V species than hydrochar, therefore, lower rate of degrading CBZ compared to hydrochar. Graphite and fullerene could not increase the decays of Fe^{VI}O₄²⁻ significantly to have enough amounts of Fe^{IV}/Fe^V species through Reactions (R5) and (R6), resulting in no enhanced degradation of CBZ (see

To further confirm the involvement of ${\rm Fe^{IV}/Fe^V}$ species through Reaction (R8) to enhance elimination of X by the ${\rm Fe^{VI}O_4}^{2-}$ -CMs system, we applied PMSO as the probe agent of high-valent iron species [35,56]. Several studies have recently been reported that the yield of PMSO₂ (η_{PMSO2}) can reflect the relative contributions of ${\rm Fe^{IV}/Fe^V}$ species [10,36,40]. We applied the PMSO as a probing agent in the ${\rm Fe^{VI}O_4}^{2-}$ -hydrochar and ${\rm Fe^{VI}O_4}^{2-}$ -GO systems. Formation of PMSO₂ from PMSO was observed (Fig. 7). The accelerated oxidation of PMSO to PMSO₂ was observed for ${\rm Fe^{VI}O_4}^{2-}$ -hydrochar and ${\rm Fe^{VI}O_4}^{2-}$ -GO systems compared to that in the oxidation by only ${\rm Fe^{VI}O_4}^{2-}$ (Fig. 7). The 100% $\eta_{\rm PMSO2}$ was consistently observed for these three systems, suggesting that ${\rm Fe^{IV}/Fe^V}$ species generated in the activated systems (Reactions (R2) and (R3)) were the oxidizing species to cause CMs-induced enhanced oxidation of X by ${\rm Fe^{VI}O_4}^{2-}$ (Reaction (R8)).

Results of Fig. 4 were comprehended by evaluating the relative reactivity of micropollutants by ${\rm Fe^{VI}O_4}^{2-}$ at pH 9.0 ($k_{\rm app}$) (Reaction (R7)). Values of the second-order rate constants of Reaction (R7) were not available for all X at pH 9.0, therefore, we used the known species-specific rate constants of involved reactants (HFe^{VI}O₄ $^ \rightleftharpoons$

 $H^{+} + Fe^{VI}O_{4}^{2-}$; $pK_{a}' = 7.23$ [57] and $HX \rightleftharpoons H^{+} + X^{-}$) to determine $k_{\mathrm{app}}.$ Rate constants including calculated k_{app} at pH 9.0 of the Reaction (R7) are given in Table 1 [21,37,58–66]. CBZ, SMX, and SDM had significant reactivity with $k_{\rm app}$ ranged from 2.7 \times 10⁰ to 6.7 \times 10⁰ M⁻¹ s⁻¹, while slow reactivity for DCF, TMP, FLU, and ATL was determined $(k_{app} = 1.2 \times 10^{0} - 7.0 \times 10^{-1} \text{ M}^{-1} \text{ s}^{-1})$. The trend in k_{app} for different X does not match with the pattern of enhanced oxidation of X by Fe^{VI}O₄²⁻-CMs (see Fig. 4). The enhanced removal of X is largely related to the occurrence of Reaction (R8) (i.e., reaction of Fe^{IV}/Fe^V species with X), with no possibility of the self-decomposition of Fe^{IV}/ Fe^V species (i.e., Reactions (R4) and (R5)). It appears that the pattern of the reactivity of Fe^{IV}/Fe^V species with X may differ from the trend of the Reaction (R7). Interestingly, the role of moieties of organic compounds in the rates of the reactions of FeV has been suggested [48,49,67]. It should also be pointed out that the self-decomposition of Fe^{VI}O₄²⁻ in alkaline medium dominated by first-order (i.e., independent of the concentration of $\mathrm{Fe^{VI}O_4}^{2-}$) and the disappearance of $\mathrm{Fe^{IV}/Fe^V}$ species are of second order at pH 9.0 (i.e., dependent on concentration) [39,48,53,68]. In other words, the relative rates of reactions of the Fe^{IV}/Fe^V species with X compared to self-decay of Fe^{IV}/Fe^V species would determine if any enhanced effect could be observed in oxidation of micropollutants by Fe^{VI}O₄²⁻-CM systems.

3.4. Recyclability of hydrochar catalyst

Hydrochar had the highest enhanced oxidation of micropollutants by Fe^{VI}O₄²⁻, therefore, the efficacy of this material was also tested for recyclability of five successive runs (Fig. SM-9). Approximately 20% decrease in enhanced oxidation of CBZ was noticed from 1st use to 2nd re-use. This decreased performance was due to the decrease in carbonyl group contents (i.e., reducing reactant) in the hydrochar that diminish the occurrence of Reaction (R3) (see Fig. 6). Further successive uses of hydrochar showed additional decrease by only ~ 5% without any influence of the number of reuses. Significantly, the reused hydrochar still showed the enhanced effect with only decrease by $\sim 30\%$ (or removal was still $\sim 70\%$) even after four successive runs of hydrochar. It appears that the reuse of the carbonaceous material could still generate the reactive Fe^{IV}/Fe^V species in the possible Reactions (R2) and (R3) to induce enhanced effect of the oxidation of CBZ by Fe^{VI}O₄²⁻. This was due to the formed Fe(III) oxide from Fe^{VI}O₄²⁻, which could be possibly adsorbed onto oxidized hydrochar and act as a catalyst to cause an enhanced effect for pollutant removal. This is supported by independent studies demonstrating the enhanced effect in the combination of FeVIO₄²⁻ with Fe(III) compared to FeVIO₄²⁻ alone [69]. In summary, Fe(III), produced from the reduction of Fe^{VI}O₄²⁻, has advantageous property to enhance the oxidation of pollutants.

4. Conclusions

Among the studied CMs (i.e., GO, hydrochar, rGO, graphite, and fullerene), GO and hydrochar had the enhanced oxidation of

micropollutants by ${\rm Fe^{VI}O_4}^{2-}$ under slightly alkaline medium. An increase in amounts of ${\rm Fe^{VI}O_4}^{2-}$ and CMs in solution of ${\rm Fe^{VI}O_4}^{2-}$ -GO (or hydrochar)-micropollutants showed generally the faster removal of micropollutants. Furthermore, the enhanced removal of micropollutants was more in using hydrochar than GO as carbonaceous material. This observation could be related to the surface functionality of the materials. The possible reactions involved and their rates in the mixture of ${\rm Fe^{VI}O_4}^{2-}$, GO (or hydrochar), and micropollutant reasonably explained the enhanced oxidation of micropollutants. The high-valent iron-oxo intermediates $({\rm Fe^{IV}/Fe^{V}})$ were invoked to describe the accelerating removal of micropollutants. Significantly, the magnitude of enhanced removal of micropollutants depended on the structure (or moieties) of micropollutants, which may have to react significantly with the high valent iron species $({\rm Fe^{IV}/Fe^{V}})$ to cause the enhanced effect due to CMs.

Declaration of Competing Interest

The authors declare that they have no known competing financial interests or personal relationships that could have appeared to influence the work reported in this paper.

Acknowledgments

V.K. Sharma and C.-H. Huang acknowledge the support from National Science Foundation (CBET 1802944 and CBET 1802800). We thank anonymous reviewers for their comments, which improved the paper.

Appendix A. Supplementary data

Supplementary data to this article can be found online at https://doi.org/10.1016/j.cej.2020.125607.

References

- J.C. Védrine, Metal oxides in heterogeneous oxidation catalysis: state of the art and challenges for a more sustainable world, ChemSusChem 12 (2019) 577–588.
- [2] Z. Tang, Y. Liu, M. He, W. Bu, Chemodynamic therapy: tumour microenvironment-mediated fenton and fenton-like reactions, Angew. Chem. Int. Ed. 58 (2019) 946–956.
- [3] M. Guo, T. Corona, K. Ray, W. Nam, Heme and nonheme high-valent iron and manganese oxo cores in biological and abiological oxidation reactions, ACS Cent. Sci. 5 (2019) 13–28.
- [4] V. Dantignana, J. Serrano-Plana, A. Draksharapu, C. Magallón, S. Banerjee, R. Fan, I. Gamba, Y. Guo, L. Que, M. Costas, A. Company, Spectroscopic and reactivity comparisons between nonheme oxoiron(IV) and oxoiron(V) species bearing the same ancillary ligand, J. Am. Chem. Soc. 141 (2019) 15078–15091.
- [5] G.R. Warner, Y. Somasundar, K.C. Jansen, E.Z. Kaaret, C. Weng, A.E. Burton, M.R. Mills, L.Q. Shen, A.D. Ryabov, G. Pros, T. Pintauer, S. Biswas, M.P. Hendrich, J.A. Taylor, F.S. Vom Saal, T.J. Collins, Bioinspired, multidisciplinary, iterative catalyst design creates the highest performance peroxidase mimics and the field of sustainable ultradilute oxidation catalysis (SUDOC), ACS Catal. 9 (2019) 7023–7037
- [6] F. Meng, C. Baum, N. Nesnas, Y. Lee, C. Huang, V.K. Sharma, Oxidation of sulfonamide antibiotics of six-membered heterocyclic moiety by ferrate(VI): kinetics and mechanistic insight into SO₂ extrusion, Environ. Sci. Technol. 53 (2019) 2695–2704
- [7] X. Lu, X-. Li, Y-. Lee, Y. Jang, M.S. Seo, S. Hong, K-. Cho, S. Fukuzumi, W. Nam, Electron-transfer and redox reactivity of high-valent iron imido and oxo complexes with the formal oxidation states of five and six, J. Am. Chem. Soc. 142 (2020) 3891–3904.
- [8] S. Xu, A. Draksharapu, W. Rasheed, L. Que, Acid p Ka dependence in O-O bond heterolysis of a nonheme FeIII-OOH intermediate to form a potent FeV = O oxidant with heme compound I-like reactivity, J. Am. Chem. Soc. 141 (2019) 16093–16107.
- [9] H. Su, C. Yu, Y. Zhou, L. Gong, Q. Li, P.J.J. Alvarez, M. Long, Quantitative structureactivity relationship for the oxidation of aromatic organic contaminants in water by TAML/H2O2, Water Res. 140 (2018) 354–363.
- [10] B. Shao, H. Dong, B. Sun, X. Guan, Role of ferrate(IV) and ferrate(V) in activating ferrate(VI) by calcium sulfite for enhanced oxidation of organic contaminants, Environ. Sci. Technol. 53 (2019) 894–902.
- [11] V.K. Sharma, R. Zboril, R.S. Varma, Ferrates: greener oxidants with multimodal action in water treatment technologies, Acc. Chem. Res. 48 (2015) 182–191.
- [12] J.E. Goodwill, J. LaBar, D. Slovikosky, W.H.J. Strosnider, Preliminary assessment of ferrate treatment of metals in acid mine drainage, J. Environ. Qual. 48 (2019) 1549–1556.

- [13] H. Liu, J. Chen, N. Wu, X. Xu, Y. Qi, L. Jiang, X. Wang, Z. Wang, Oxidative degradation of chlorpyrifos using ferrate(VI): Kinetics and reaction mechanism, Ecotoxicol. Environ. Saf. 170 (2019) 259–266.
- [14] F. Dong, J. Liu, C. Li, Q. Lin, T. Zhang, K. Zhang, V.K. Sharma, Ferrate(VI) pretreatment and subsequent chlorination of blue-green algae: Quantification of disinfection byproducts, Environ. Int. 133 (2019).
- [15] X. Sun, Q. Zhang, H. Liang, L. Ying, M. Xiangxu, V.K. Sharma, Ferrate(VI) as a greener oxidant: electrochemical generation and treatment of phenol, J. Hazard. Mater. 319 (2016) 130–136.
- [16] Y. Liu, J. Zhang, H. Huang, Z. Huang, C. Xu, G. Guo, H. He, J. Ma, Treatment of trace thallium in contaminated source waters by ferrate pre-oxidation and poly aluminium chloride coagulation, Sep. Purif. Technol. 227 (2019).
- [17] R. Prucek, J. Tucek, J. Kolarik, İ. Huskova, J. Filip, R.S. Varma, V.K. Sharma, R. Zboril, Ferrate(VI)-prompted removal of metals in aqueous media: mechanistic delineation of enhanced efficiency via metal entrenchment in magnetic oxides, Environ. Sci. Technol. 49 (2015) 2319–2327.
- [18] K. Manoli, R. Maffettone, V.K. Sharma, D. Santoro, A.K. Ray, K.D. Passalacqua, K.E. Carnahan, C. Wobus, S. Sarathy, Inactivation of murine norovirus and fecal coliforms by ferrate(VI) in secondary effluent wastewater, Enviorn. Sci. Technol. 54 (2020) 1878–1888.
- [19] V.K. Sharma, L. Chen, R. Zboril, Review on high valent Fe^{VI} (ferrate): A sustainable green oxidant in organc chemistry and transformation of pharmaceuticals, ACS Sustainable Chem. Eng. 4 (2016) 18–34.
- [20] A. Karlesa, G.A.D. De Vera, M.C. Dodd, J. Park, M.P.B. Espino, Y. Lee, Ferrate(VI) oxidation of ß-lactam antibiotics: Reaction kinetics, antibacterial activity changes, and transformation products, Environ. Sci. Technol. 48 (2014) 10380–10389.
- [21] Y. Lee, S.G. Zimmermann, A.T. Kieu, U. von Gunten, Ferrate (Fe(VI)) application for municipal wastewater treatment: a novel process for simultaneous micropollutant oxidation and phosphate removal, Environ. Sci. Technol. 43 (2009) 3831–3838.
- [22] T. Yang, L. Wang, Y. Liu, Z. Huang, H. He, X. Wang, J. Jiang, D. Gao, J. Ma, Comparative study on ferrate oxidation of BPS and BPAF: Kinetics, reaction mechanism, and the improvement on their biodegradability, Water Res. 148 (2019) 115–125.
- [23] J. Chen, X. Xu, X. Zeng, M. Feng, R. Qu, Z. Wang, N. Nesnas, V.K. Sharma, Ferrate (VI) oxidation of polychlorinated diphenyl sulfides: Kinetics, degradation, and oxidized products. Water Res. 143 (2018) 1–9.
- [24] J. Chen, R. Qu, X. Pan, Z. Wang, Oxidative degradation of triclosan by potassium permanganate: Kinetics, degradation products, reaction mechanism, and toxicity evaluation, Water Res. 103 (2016) 215–223.
- [25] Z-. Huang, L. Wang, Y-. Liu, J. Jiang, M. Xue, C-. Xu, Y-. Zhen, Y-. Wang, J. Ma, Impact of phosphate on ferrate oxidation of organic compounds: an underestimated oxidant, Environ. Sci. Technol. 52 (2018) 13897–13907.
- [26] M. Feng, L. Cizmas, Z. Wang, V.K. Sharma, Synergistic effect of aqueous removal of fluoroquinolones by a combined use of peroxymonosulfate and ferrate(VI), Chemosphere 177 (2017) 144–148.
- [27] M. Ghosh, K. Manoli, J.B. Renaud, L. Sabourin, G. Nakhla, V.K. Sharma, A.K. Ray, Rapid removal of acesulfame potassium by acid-activated ferrate(VI) under mild alkaline conditions, Chemosphere 230 (2019) 416–423.
- [28] K. Manoli, L.M. Morrison, M.W. Sumarah, G. Nakhla, A.K. Ray, V.K. Sharma, Pharmaceuticals and pesticides in secondary effluent wastewater: Identification and enhanced removal by acid-activated ferrate(VI), Water Res. 148 (2019) 272–280.
- [29] S. Sun, S. Pang, J. Jiang, J. Ma, Z. Huang, J. Zhang, Y. Liu, C. Xu, Q. Liu, Y. Yuan, The combination of ferrate(VI) and sulfite as a novel advanced oxidation process for enhanced degradation of organic contaminants, Chem. Eng. J. 333 (2018) 11–19.
- [30] M. Feng, C. Jinadatha, T.J. McDonald, V.K. Sharma, Accelerated oxidation of organic contaminants by ferrate(VI): the overlooked role of reducing additives, Environ. Sci. Technol. 52 (2018) 11319–11327.
- [31] K. Manoli, G. Nakhla, A.K. Ray, V.K. Sharma, Enhanced oxidative transformation of organic contaminants by activation of ferrate(VI): possible involvement of FeV/ FeIV species, Chem. Eng. J. 307 (2017) 513–517.
- [32] V.K. Sharma, Ferrate(V) oxidation of pollutants: a premix pulse radiolysis, Radiat. Phys. Chem. 65 (2002) 349–355.
- [33] R.J. Terryn, C.A. Huerta-Aguilar, J.C. Baum, V.K. Sharma, FeVI, FeV, and FeIV oxidation of cyanide: elucidating the mechanism using density functional theory calculations, Chem. Eng. J. 330 (2017) 1272–1278.
- [34] N.N. Noorhasan, V.K. Sharma, D. Cabelli, Reactivity of ferrate(V) (FeVO43-) with aminopolycarboxylates in alkaline medium: a premix pulse radiolysis, Inorg. Chim. Acta 361 (2008) 1041–1046.
- [35] B. Shao, H. Dong, L. Feng, J. Qiao, X. Guan, Influence of [sulfite]/[Fe(VI)] molar ratio on the active oxidants generation in Fe(VI)/sulfite process, J. Hazard. Mater. 384 (2020).
- [36] C. Luo, M. Feng, V.K. Sharma, C-. Huang, Oxidation of pharmaceuticals by ferrate (VI) in hydrolyzed urine: effects of major inorganic constituents, Environ. Sci. Technol. 53 (2019) 5272–5281.
- [37] M. Feng, L. Cizmas, Z. Wang, V.K. Sharma, Activation of ferrate(VI) by ammonia in oxidation of flumequine: kinetics, transformation products, and antibacterial activity assessment, Chem. Eng. J. 323 (2017) 584–591.
- [38] K. Manoli, G. Nakhla, M. Feng, V.K. Sharma, A.K. Ray, Silica gel-enhanced oxidation of caffeine by ferrate(VI), Chem. Eng. J. 330 (2017) 987–994.
- [39] C. Luo, M. Feng, V.K. Sharma, C-. Huang, Revelation of ferrate(VI) unimolecular decay under alkaline conditions: investigation of involvement of Fe(IV) and Fe(V) species, Chem. Eng. J. 388 (2020).
- [40] S. Sun, J. Jiang, L. Qiu, S. Pang, J. Li, C. Liu, L. Wang, M. Xue, J. Ma, Activation of ferrate by carbon nanotube for enhanced degradation of bromophenols: kinetics, products, and involvement of Fe(V)/Fe(IV), Water Res. 156 (2019) 1–8.
- [41] Z. Luo, M. Strouse, J.Q. Jiang, V.K. Sharma, Methodologies for the analytical

- determination of ferrate(VI): a review, J. Environ. Sci. Health Part A Toxic/Hazard. Subs Environ. Eng. 46 (2011) 453–460.
- [42] J.D. Rush, B.H.J. Bielski, Pulse radiolysis studies of alkaline Fe(III) and Fe(VI) solutions. Observation of transient iron complexes with intermediate oxidation states, J. Am. Chem. Soc. 108 (1986) 523–525.
- [43] M. Sevilla, A.B. Fuertes, Chemical and structural properties of carbonaceous products obtained by hydrothermal carbonization of saccharides, Chem. Eur. J. 15 (2009) 4195–4203.
- [44] K. Aydincak, T. Yumak, A. Sinağ, B. Esen, Synthesis and characterization of carbonaceous materials from saccharides (glucose and lactose) and two waste biomasses by hydrothermal carbonization, Ind. Eng. Chem. Res. 51 (2012) 9145–9152.
- [45] H. Kim, Y.S. Hwang, V.K. Sharma, Adsorption of antibiotics and iopromide onto single-walled and multi-walled carbon nanotubes, Chem. Eng. J. 255 (2014) 23–27.
- [46] B. Peng, L. Chen, C. Que, K. Yang, F. Deng, X. Deng, G. Shi, G. Xu, M. Wu, Adsorption of antibiotics on graphene and biochar in aqueous solutions induced by p-p Interactions, Sci Rep 6 (2016) 31920.
- [47] C.A. Sophia, E.C. Lima, Removal of emerging contaminants from the environment by adsorption, Ecotoxicol. Environ. Saf. 150 (2018) 1–17.
- [48] B.H.J. Bielski, V.K. Sharma, G. Czapski, Reactivity of ferrate(V) with carboxylic acids: a pre-mix pulse radiolysis study, Radiat. Phys. Chem. 44 (1994) 479–484.
- [49] V.K. Sharma, B.H.J. Bielski, Reactivity of ferrate(VI) and ferrate(V) with amino acids, Inorg. Chem. 30 (1991) 4306–4311.
- [50] J.D. Carr, Kinetics and product identification of oxidation by ferrate(VI) of water and aqueous nitrogen containing solutes, ACS Symp. Ser. 985 (Ferrates) (2008) 189–196.
- [51] V.K. Sharma, Potassium ferrate(VI): Environmental friendly oxidant, Adv. Environ. Res. 6 (2002) 143–156.
- [52] R. Bartzatt, J. Carr, The kinetics of oxidation of low molecular weight aldehydes by potassium ferrate, Trans. Met. Chem. 11 (1986) 414–416.
- [53] J.D. Rush, B.H.J. Bielski, Decay of ferrate(V) in neutral and acidic solutions. A premix pulse radiolysis study, Inorg. Chem. 33 (1994) 5499–5502.
- [54] J.D. Rush, B.H.J. Bielski, Kinetics of ferrate(V) decay in aqueous solution. A pulseradiolysis study, Inorg. Chem. 28 (1989) 3947–3951.
- [55] V.K. Sharma, Oxidation of inorganic contaminants by ferrates(Fe(VI), Fe(V), and Fe (IV))-kinetics and mechanisms – A Review, J. Environ. Manage. 92 (2011) 1051–1073.
- [56] H. Li, C. Shan, W. Li, B. Pan, Peroxymonosulfate activation by iron(III)-tetraamidomacrocyclic ligand for degradation of organic pollutants via high-valent iron-

- oxo complex, Water Res. 147 (2018) 233-241.
- [57] V.K. Sharma, C.R. Burnett, F.J. Millero, Dissociation constants of monoprotic ferrate (VI) ions in NaCl media, Phys. Chem. Chem. Phys. 3 (2001) 2059–2062.
- [58] V.K. Sharma, S.K. Mishra, A.K. Ray, Kinetic assessment of the potassium ferrate(VI) oxidation of antibacterial drug sulfamethoxazole, Chemosphere 62 (2006) 129, 124
- [59] V.K. Sharma, S.K. Mishra, N. Nesnas, Oxidation of sulfonamide antimicrobials by ferrate(VI) [Fe^{VI}O₄²], Environ. Sci. Technol. 40 (2006) 7222–7227.
- [60] G.A.K. Anquandah, V.K. Sharma, D.A. Knight, S.R. Batchu, P.R. Gardinali, Oxidation of trimethoprim by ferrate(VI): kinetics, products, and antibacterial activity, Environ. Sci. Technol. 45 (2011) 10575–10581.
- [61] Y. Lee, U. von Gunten, Oxidative transformation of micropollutants during municipal wastewater treatment: comparison of kinetic aspects of selective (chlorine, chlorine dioxide, ferrate^{VI}, and ozone) and non-selective oxidants (hydroxyl radical), Water Res. 44 (2010) 555–566.
- [62] A.L. Boreen, W.A. Arnold, K. McNeill, Photochemical fate of sulfa drugs in then aquatic environment: sulfa drugs containing five-membered heterocyclic groups, Environ. Sci. Technol. 38 (2004) 3933–3940.
- [63] A.L. Boreen, W.A. Arnold, K. McNeill, Triplet-sensitized photodegradation of sulfa drugs containing six-membered heterocyclic groups: Identification of an SO2 extrusion photoproduct, Environ. Sci. Technol. 39 (2005) 3630–3638.
- [64] B. Roth, J.Z. Strelitz, Protonation of 2,4-diaminopyrimidines. I. Dissociation constants and substituent effects, J. Org. Chem. 34 (1969) 821–836.
- [65] M.M. Huber, S. Canonica, G.Y. Park, U. Von Gunten, Oxidation of pharmaceuticals during ozonation and advanced oxidation processes, Environ. Sci. Technol. 37 (2003) 1016–1024.
- [66] H. Park, T.H. Kim, K. Bark, Physicochemical properties of quinolone antibiotics in various environments, Eur. J. Med. Chem. 37 (2002) 443–460.
- [67] B.H.J. Bielski, M.J. Thomas, Studies of hypervalent iron in aqueous solutions. 1. Radiation-induced reduction of iron(VI) to iron(V) by CO₂, J. Amer. Chem. Soc. 109 (1987) 7761–7764
- [68] J.D. Menton, B.H.J. Bielski, Studies of the kinetics, spectral and chemical properties of Fe(IV) pyrophosphate by pulse radiolysis, Radiat. Phys. Chem. 36 (1990) 725–733.
- [69] J. Zhao, Y. Liu, Q. Wang, Y. Fu, X. Lu, X. Bai, The self-catalysis of ferrate (VI) by its reactive byproducts or reductive substances for the degradation of diclofenac: kinetics, mechanism and transformation products, Sep. Purif. Technol. 192 (2018) 412–418.